

Hyperfine structure of the $2p^2P_{1/2}$ state in ${}^9\text{Be}^+$

J. J. Bollinger, J. S. Wells, D. J. Wineland, and Wayne M. Itano

*Time and Frequency Division, National Bureau of Standards,
Boulder, Colorado 80303*

(Received 17 October 1984)

An optical-optical double resonance technique has been used on beryllium ions stored in a Penning trap to measure the magnetic dipole hyperfine interaction constant $A_{1/2}$ of the $2p^2P_{1/2}$ level in ${}^9\text{Be}^+$. The measured value of $A_{1/2} = -118.6(3.6)$ MHz is in good agreement with theoretical calculations. The $2p^2P$ fine-structure splitting and the $2s^2S_{1/2} \rightarrow 2p^2P_{3/2,1/2}$ optical transition frequencies have also been measured.

The $2p^2P$ hyperfine structure of the LiI electronic sequence has attracted much theoretical interest over the past two decades (see, for example, Refs. 1–4 and references contained in Ref. 5). This is because of the computational feasibility in a three-electron system, the importance of and interest in polarization and correlation effects, and the availability of good experimental measurements^{5–7} in ${}^7\text{Li}$. The $A_{1/2}$, $A_{3/2}$, and $A_{3/2,1/2}$ hyperfine constants of the $2p^2P$ state in ${}^7\text{Li}$ have been measured; these constants determine the individual spin-dipolar, orbital, and contact contributions to the $2p^2P$ hyperfine structure. Agreement with theoretical calculations is on the order of a few percent.¹ Measurements of the $A_{3/2}$ hyperfine constant of the $2p^2P$ state have been made in ${}^9\text{Be}^+$ (Ref. 8) and ${}^{11}\text{B}^{2+}$ (Ref. 9). In ${}^9\text{Be}^+$, $|A_{3/2}|$ has been measured to be less than 0.6 MHz.⁸ A Hartree-Fock central field calculation yields the value $A_{3/2} \cong -18.7$ MHz, but polarization and correlation effects contribute +17.2 MHz and produce a final value of $A_{3/2} = -1.5(1.2)$ MHz in agreement with the experimental measurements.¹ Measurements of the $A_{1/2}$ and $A_{3/2,1/2}$ hyperfine constants of the $2p^2P$ state in ${}^9\text{Be}^+$ are useful for further tests of the theoretical calculations and are needed to determine the individual spin-dipolar, orbital, and contact contributions to the $2p^2P$ hyperfine structure. This paper reports the first measurement of the $A_{1/2}$ hyperfine constant of the $2p^2P$ state in ${}^9\text{Be}^+$. The measured value of $A_{1/2} = -118.6(3.6)$ MHz is in agreement with the theoretical calculation of Ref. 1 of $-116.8(2.4)$ MHz.

Much of the experimental apparatus used in this measurement has been described in other reports.^{10,11} ${}^9\text{Be}^+$ ions were confined by the static magnetic and electric fields of a Penning trap in ultrahigh vacuum ($< 10^{-7}$ Pa). The uniform magnetic field of approximately 1.1 T nearly decoupled the nuclear spin from the total electronic angular momentum. The confining electric field (≤ 1 V/cm) had a negligible perturbation (< 1 Hz) on the $2s^2S_{1/2}$ and $2p^2P_J$ energy levels of the ions. The benign environment and long confinement times of electromagnetic traps have been used to make numerous high-precision rf and microwave measurements of the hyperfine structure in the ground state of ions.¹² Here, however, an optical measurement of the first excited state hyperfine structure was accomplished by using laser cooling to reduce the ion temperature below a few K so that the hyperfine components of the optical transition were resolved. A narrow-band (< 4 MHz) radiation source (power $\cong 20$ μW) tuned to the low-frequency side of the

$$2s^2S_{1/2}(M_I, M_J) = (-\frac{3}{2}, -\frac{1}{2}) \rightarrow 2p^2P_{3/2}(-\frac{3}{2}, -\frac{3}{2})$$

($\lambda = 313$ nm)

transition of ${}^9\text{Be}^+$ was used to cool and spatially compress the ions and optically pump them into the $(-\frac{3}{2}, -\frac{1}{2})$ ground state.¹¹ The 313-nm source was obtained by frequency doubling the output of a single-mode cw dye laser. The resonance fluorescence induced by this “cooling” laser was used to detect the ions.¹¹ Typical ion “clouds” consisted of at most several hundred ions with cloud densities of 2×10^7 ions/cm³ and cloud diameters of 100–300 μm .

The $2p^2P_{1/2}$ hyperfine structure was measured by an optical-optical double resonance technique with a second frequency-doubled dye laser, denoted the probe laser (power $\ll 1$ μW).¹³ When the probe laser was tuned in resonance with the

$$2s^2S_{1/2}(-\frac{3}{2}, -\frac{1}{2}) \rightarrow 2p^2P_{1/2}(-\frac{3}{2}, +\frac{1}{2})$$

transition (transition A), some of the ion population was removed from the $(-\frac{3}{2}, -\frac{1}{2})$ ground state. This resulted in a decrease in the observed fluorescence induced by the cooling laser. The $2s^2S_{1/2}(-\frac{3}{2}, -\frac{1}{2}) \rightarrow 2p^2P_{1/2}(-\frac{3}{2}, -\frac{1}{2})$ transition (transition B) was detected in a similar way. Radio-frequency (rf) radiation (frequency approximately equal to 300 MHz) tuned to the ground-state $(-\frac{3}{2}, -\frac{1}{2}) \rightarrow (-\frac{1}{2}, -\frac{1}{2})$ transition was used to mix the $(-\frac{3}{2}, -\frac{1}{2})$ and $(-\frac{1}{2}, -\frac{1}{2})$ ground states. Owing to this rf mixing, a decrease in the fluorescent light intensity was also observed when the probe laser was tuned from the $(-\frac{1}{2}, -\frac{1}{2})$ ground state to the $2p^2P_{1/2}(-\frac{1}{2}, +\frac{1}{2})$ state (transition C). Figure 1 shows the transitions driven by the probe laser. Figure 2(a) shows the depopulation signals obtained when the probe laser was frequency swept through transitions A and C.

Part of the probe dye laser beam, before doubling, was picked off and sent into an ${}^{127}\text{I}_2$ cell. ${}^{127}\text{I}_2$ saturated absorption spectra were simultaneously recorded as the probe laser was frequency swept through the optical transitions to the $2p^2P_{1/2}$ state (see Fig. 2). At the magnetic field used in this experiment, line number 955 of the ${}^{127}\text{I}_2$ atlas¹⁴ and the next higher-frequency line (uncataloged) approximately coincided with the ${}^9\text{Be}^+$ transitions to the $M_J = -\frac{1}{2}$ and $M_J = +\frac{1}{2}$ states of the $2p^2P_{1/2}$ manifold, respectively. The frequency differences between the I_2 hyperfine components were measured by stabilizing two dye lasers to different I_2 hyperfine components and making heterodyne difference frequency measurements on a p - i - n diode. This provided the frequency scale from which measurements of the frequency differences between the transitions detected by the

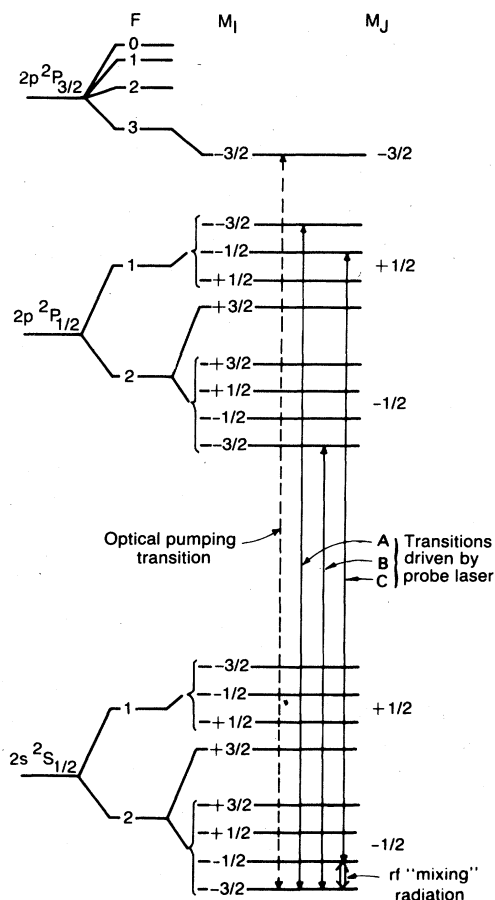


FIG. 1. Sketch of the energy levels of the $2s^2S_{1/2}$ and $2p^2P_{1/2}$ states of Be^+ . The cooling/optical pumping transition is indicated by the dotted line. The transitions detected by the probe laser are marked by solid lines and are labeled A, B, and C. The rf mixing radiation serves to populate both the $(M_I, M_J) = (-\frac{3}{2}, -\frac{1}{2})$ and $(-\frac{1}{2}, -\frac{1}{2})$ ground states.

probe laser were made. From data like that shown in Fig. 2, the frequency difference between transitions A and C was measured to be 360.4(2.4) MHz. (Error estimates in this paper are one standard deviation uncertainties.) The measured frequency difference between transitions A and B was 10787.7(5.4) MHz. In addition to random error, the error estimates include uncertainties in systematic shifts due to background slopes, overlap of neighboring transitions, and calibration of the frequency scale. By alternately chopping the probe and cooling laser beams (at about 30 Hz), potential light shifts were eliminated. Any ac Stark or ac Zeeman shifts produced by the ground-state rf mixing were estimated to be negligible.

The 360.4(2.4)-MHz difference between transitions A and C is the sum of $2p^2P_{1/2}$ hyperfine-structure contributions and the $(-\frac{3}{2}, -\frac{1}{2}) \rightarrow (-\frac{1}{2}, -\frac{1}{2})$ ground-state splitting. The ground-state contribution was separately measured by an rf-optical double resonance technique^{10,11} to be 310.286 815(30) MHz. The splitting between the $2p^2P_{1/2}(-\frac{3}{2}, +\frac{1}{2})$ and $2p^2P_{1/2}(-\frac{1}{2}, +\frac{1}{2})$ states is then 50.1(2.4) MHz. In addition, the measured value of the

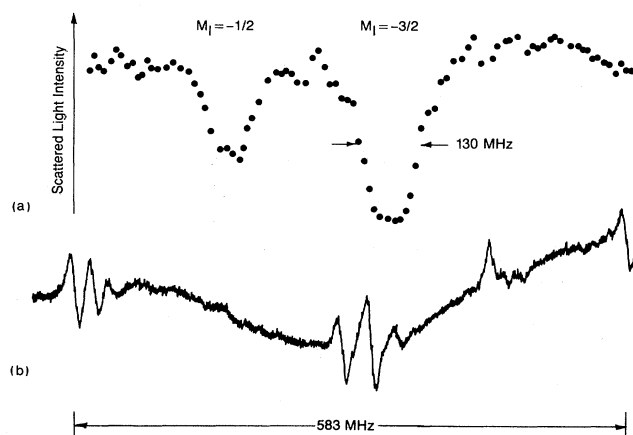


FIG. 2. (a) Depopulation signals obtained when the probe laser was frequency swept through transitions A and C. The data are the average of eight sweeps. (b) $^{127}\text{I}_2$ saturated absorption spectra ($^{127}\text{I}_2$ scattered light intensity vs frequency) simultaneously recorded with the depopulation signals. The frequency scale of the $^{127}\text{I}_2$ saturated absorption spectra is half the frequency scale of the $^9\text{Be}^+$ depopulation signals. These $^{127}\text{I}_2$ hyperfine components belong to the next higher frequency line (uncataloged) above line number 955 in the $^{127}\text{I}_2$ atlas (see Ref. 14).

$(-\frac{3}{2}, -\frac{1}{2}) \rightarrow (-\frac{1}{2}, -\frac{1}{2})$ ground-state transition was used, along with measured values of the ground-state hyperfine constant and g factors,^{10,15} to determine the magnetic field, $B = 1.136\,827\,7(22)$ T.

The absolute frequencies of the optical $2s^2S_{1/2} \leftrightarrow 2p^2P_{1/2}$ transitions were determined (to less precision than the frequency differences) from the simultaneous recordings of the $^9\text{Be}^+$ signals and the $^{127}\text{I}_2$ saturated absorption signals along with the tabulated frequencies¹⁴ of the $^{127}\text{I}_2$ lines. Transitions A, B, and C were measured relative to line number 954 [R91(3-8)] of the $^{127}\text{I}_2$ atlas because it was the nearest unblended line. Similarly, the $2s^2S_{1/2}(-\frac{3}{2}, -\frac{1}{2}) \rightarrow 2p^2P_{3/2}(-\frac{3}{2}, -\frac{3}{2})$ cooling transition was also measured relative to line number 960 [P89(4-10)]. These measurements, along with the measured magnetic field, the ground-state hyperfine constant and g factors,^{10,15} and the Landé g factors for the $2p^2P_{1/2}$ and $2p^2P_{3/2}$ states, determine the $2p^2P$ zero-field fine-structure interval ΔE , and the $2s^2S_{1/2} \leftrightarrow 2p^2P_{1/2}$ and $2s^2S_{1/2} \leftrightarrow 2p^2P_{3/2}$ zero-field optical transition frequencies. We obtained

$$\Delta E/h = 197\,150(64) \text{ MHz} ,$$

$$\nu(2s^2S_{1/2} \leftrightarrow 2p^2P_{1/2}) = 31\,928.7436(40) \text{ cm}^{-1} ,$$

$$\nu(2s^2S_{1/2} \leftrightarrow 2p^2P_{3/2}) = 31\,935.3198(45) \text{ cm}^{-1} .$$

These values agree with the previous, less precise measurements of Ref. 16. A many-body perturbation theory calculation^{17,18} of $\Delta E/h = 6.412 \text{ cm}^{-1} = 192\,227 \text{ MHz}$ is within 2.5% of the experimental measurement.

The Hamiltonian for the $2p^2P$ manifold is given by

$$H = H_{fs} + H_{Ze} + H_{Zn} + H_{hfs} + H'_{Ze} .$$

$H_{fs} = (\frac{2}{3})\Delta E L \cdot S$ is the fine-structure interaction. $H_{Ze} = (g_L L_z + g_S S_z)\mu_B B$ is the Zeeman interaction of the exter-

nal magnetic field with the electron orbital and spin magnetic moments. We take $g_S = 2.0023193$ (free-electron value) and $g_L = 1$ (reduced mass corrections are included in H'_{Ze}). $H_{Zn} = -g_I \mu_N I_z B$ is the Zeeman interaction of the external magnetic field with the nuclear magnetic moment. μ_B and μ_N are the Bohr and nuclear magnetons. g_I is the nuclear g factor in the $2p^2P$ state of ${}^9\text{Be}^+$. For the precision of these measurements, g_I can be taken equal to the g factor of the bare nucleus,¹⁹ $g_I = -0.784955(2)$. H_{hfs} is the hyperfine-structure interaction. $H_{\text{hfs}} = H_{\text{hfsm}} + H_Q$ consists of a magnetic dipole interaction H_{hfsm} and an electric quadrupole interaction H_Q . The electric quadrupole interaction does not couple the nuclear quadrupole moment with the $2p^2P_{1/2}$ states and, for the purposes of this experiment, can be neglected. H_{hfsm} can be parametrized by the three constants^{1,5}

$$A_J = \frac{\langle J, M_J = J, I, M_I = I | H_{\text{hfsm}} | J, M_J = J, I, M_I = I \rangle}{hIJ}$$

$$= \frac{\langle J, M_J = J, I, M_I = I | hA_I \mathbf{I} \cdot \mathbf{J} | J, M_J = J, I, M_I = I \rangle}{hIJ},$$

for $J = \frac{3}{2}, \frac{1}{2}$, and the off-diagonal element

$$A_{J, J-1} = \frac{\langle J, M_J, I, M_I | H_{\text{hfsm}} | J-1, M_J, I, M_I \rangle}{hM_I(J^2 - M_I^2)^{1/2}},$$

$$(E_{-3/2, 1/2} - E_{-1/2, 1/2})/h = 50.1(2.4) \text{ MHz (experiment)}$$

$$= -(1 - \alpha^2)A_{1/2}/2 - A_{1/2}^2/4U + \alpha 2\sqrt{2}A_{3/2, 1/2} + g_I \mu_N B/h, \quad (1)$$

$$(E_{-3/2, 1/2} - E_{-3/2, -1/2})/h = 10787.7(5.4) \text{ MHz (experiment)}$$

$$= U + \delta g_{1/2} \mu_B B/h - 3[1 - (\alpha^2 + \beta^2)/2]A_{1/2}/2 + 3A_{1/2}^2/4U + (\alpha - \beta)3\sqrt{2}A_{3/2, 1/2}. \quad (2)$$

$\delta g_{1/2}$ is the sum of the corrections to the $2p^2P_{1/2}$ g_J factor due to H'_{Ze} . Its value was calculated by many-body perturbation theory to be $-10.95(3) \times 10^{-5}$.¹⁸

The quantity $A_{1/2} = -118.6(3.6)$ MHz was determined from Eqs. (1) and (2) and is in good agreement with the theoretical calculation of $A_{1/2} = -116.8(2.4)$ MHz.¹ The uncertainty is due mainly to the experimental uncertainty in the measured frequencies. A rather poor value for $A_{3/2, 1/2}$ of $A_{3/2, 1/2} = -19.2(28.6)$ MHz was also determined from Eqs. (1) and (2). The calculation of Ref. 1 predicts $A_{3/2, 1/2} = -23.2(1.0)$ MHz. The precision of the $A_{3/2, 1/2}$ measurement was limited by the small 0.04 amplitude admixture of the $2p^2P_{3/2}$ states in the $2p^2P_{1/2}$ manifold.

Increased accuracy in the hyperfine constants and an independent determination of the $2p^2P_{1/2}$ g_J factor can be obtained by measuring more transitions at higher magnetic

for $J = \frac{3}{2}$. H'_{Ze} is the relativistic, diamagnetic, and finite nuclear mass correction to the Zeeman interaction H_{Ze} .^{20,21}

If H_{Zn} , H_{hfs} , and H'_{Ze} are at first neglected, the energies and eigenstates of $H_{\text{fs}} + H_{Ze}$ can be determined analytically. Let $|J, M_J\rangle$ denote an eigenstate of J^2 and J_z . The $2p^2P_{1/2}$ $M_J = +\frac{1}{2}$ and $M_J = -\frac{1}{2}$ eigenstates of $H_{\text{fs}} + H_{Ze}$ are, respectively,

$$(1 - \alpha^2)^{1/2} |\frac{1}{2}, \frac{1}{2}\rangle - \alpha |\frac{3}{2}, \frac{1}{2}\rangle$$

and

$$(1 - \beta^2)^{1/2} |\frac{1}{2}, -\frac{1}{2}\rangle - \beta |\frac{3}{2}, -\frac{1}{2}\rangle.$$

With the experimental values $B = 1.1368277(22)$ T and $(\Delta E/h) = 197150(64)$ MHz, the theoretically determined $J = \frac{3}{2}$ amplitude admixtures are $\alpha = 0.03706(1)$ and $\beta = 0.03910(1)$, and the states are theoretically split by a frequency $U = 10610.57(1)$ MHz. The effects of $H_{Zn} + H_{\text{hfsm}} + H'_{Ze}$ were treated by perturbation theory. Terms with estimated contributions of much less than 0.1 MHz were neglected. The following two equations were obtained for the measured frequency differences, $(E_{M_I, M_J} - E_{M'_I, M'_J})/h$, in the $2p^2P_{1/2}$ manifold:

fields. At approximately 6.26 T, the $2p^2P_{3/2}$, $M_J = -\frac{3}{2}$ and $2p^2P_{1/2}$, $M_J = +\frac{1}{2}$ levels cross and the $2p^2P_{3/2}$ amplitude admixture in the $2p^2P_{1/2}$ manifold is approximately 4.5 times larger than at 1.1 T. At a magnetic field of approximately 9.39 T, the $2p^2P_{3/2}$, $M_J = -\frac{3}{2}$ and $2p^2P_{1/2}$, $M_J = -\frac{1}{2}$ levels cross and the hyperfine interaction strongly couples states with $\Delta M_I = -\Delta M_J$. These antilevel crossings are particularly sensitive to the off diagonal hyperfine constant $A_{3/2, 1/2}$.^{5,6}

We gratefully acknowledge the support of the U.S. Air Force Office of Scientific Research and the U.S. Office of Naval Research. We thank J. D. Prestage and R. Blatt for carefully reading the manuscript and for helpful comments.

¹S. Garpman, I. Lindgren, J. Lindgren, and J. Morrison, *Z. Phys. A* **276**, 167 (1976); *Phys. Rev. A* **11**, 758 (1975).

²D. R. Beck and C. A. Nicolaidis, in *The Fourth International Conference on Beam-Foil Spectroscopy, September 15-19, 1975, Gatlinburg, Tennessee*, edited by I. A. Sellin and D. J. Pegg (Plenum, New York, 1976), Vol. 2, p. 105.

³R. K. Nesbet, *Phys. Rev. A* **2**, 661 (1970).

⁴J. D. Lyons, R. T. Pu, and T. P. Das, *Phys. Rev.* **178**, 103 (1969).

⁵H. Orth, H. Ackermann, and E. W. Otten, *Z. Phys. A* **273**, 221 (1975).

⁶K. C. Brog, T. G. Eck, and H. Wieder, *Phys. Rev.* **153**, 91 (1967); H. Wieder and T. G. Eck, *ibid.* **153**, 103 (1967).

⁷G. J. Ritter, *Can. J. Phys.* **43**, 770 (1965).

⁸O. Poulsen, T. Andersen, and N. Skouboe, *J. Phys. B* **8**, 1393 (1975).

⁹O. Poulsen, P. S. Ramanujam, and D. B. Iversen, *J. Phys. B* **8**, L450 (1975).

¹⁰D. J. Wineland, J. J. Bollinger, and W. M. Itano, *Phys. Rev. Lett.* **50**, 628 (1983); **50**, 1333(E) (1983).

¹¹W. M. Itano and D. J. Wineland, *Phys. Rev. A* **24**, 1364 (1981).

- ¹²D. J. Wineland, W. M. Itano, and R. S. Van Dyck, Jr., *Adv. At. Mol. Phys.* **19**, 135 (1983).
- ¹³D. J. Wineland, J. C. Bergquist, W. M. Itano, and R. E. Drullinger, *Opt. Lett.* **5**, 245 (1980).
- ¹⁴S. Gerstenkorn and P. Luc, *Atlas du spectre d'absorption de la molécule de l'iode entre 14 800–20 000 cm⁻¹* (Editions du CNRS, Paris, 1978); *Rev. Phys. Appl.* **14**, 791 (1979).
- ¹⁵W. M. Itano, D. J. Wineland, and J. J. Bollinger, *Bull. Am. Phys. Soc.* **28**, 780 (1983).
- ¹⁶L. Johansson, *Ark. Fys.* **20**, 489 (1961).
- ¹⁷L. Veseth, *J. Phys. B* **16**, 2913 (1983).
- ¹⁸L. Veseth (private communication).
- ¹⁹W. M. Itano, *Phys. Rev. B* **27**, 1906 (1983).
- ²⁰A. Abragam and J. H. Van Vleck, *Phys. Rev.* **92**, 1448 (1953).
- ²¹L. Veseth, *Phys. Rev. A* **22**, 803 (1980); *J. Phys. B* **16**, 2891 (1983).